

# **Influence of Varying Synthetic Routes on the Physicochemical Properties of Mg-Al-CO<sub>3</sub> and Zn-Al-CO<sub>3</sub> Hydrotalcite-Like Compounds: A Comparative Study**

*Selina Ilunakan Omonmhenle, Doctor of Chemistry*

Department of Chemistry, University of Benin,  
Ugbowo Campus, Benin City, Nigeria

*Ian James Shannon, Doctor of Chemistry*

School of Chemistry, University of Birmingham,  
Edgbaston, United Kingdom

Doi: 10.19044/esj.2019.v15n12p52      [URL:http://dx.doi.org/10.19044/esj.2019.v15n12p52](http://dx.doi.org/10.19044/esj.2019.v15n12p52)

---

## **Abstract**

Magnesium-Aluminium Carbonate Hydrotalcite-like Compound (Mg-Al-CO<sub>3</sub>-HTlc) and Zinc-Aluminium Carbonate Hydrotalcite-like Compound (Zn-Al-CO<sub>3</sub>-HTlc) with Mg/Al and Zn/Al atomic ratio 2:1 was synthesized by co-precipitation and urea hydrolysis methods. Their physicochemical properties were studied using powder X-ray diffraction (PXRD), X-ray fluorescence spectrophotometry (XRF), Fourier transform infrared (FTIR) and Thermogravimetry (TG) and Differential Thermal Analysis (DTA) involving evolved gas analysis (EGA). The PXRD of the synthesized material showed that the crystallinity is influenced by the type of synthetic method and can affect the properties of the hydrotalcite-like compounds. The TG, DTA and EGA results showed that three steps of mass loss occurred corresponding to the release of gallery water, structural water and carbon dioxide (from carbonate decomposition) respectively. Thermal treatment up to about 500°C and beyond transforms them into non-stoichiometric metal stable oxides (MgO and ZnO) whose crystallinity is lower than that of the precursor and then into stable spinel with no further mass loss following the transformation. Derivatives of urea hydrolysis method gave better ordered and more crystalline Mg<sub>2</sub>AlCO<sub>3</sub>-HTlc but with smaller unit cell. Variation in synthesis route can influence the mode of stacking of the layers, order of the interlayer anions and water molecules in the gallery space and attraction between the interlayer anions and the hydroxyl ions of the metal hydroxide layers.

**Keywords:** Hydrotalcite-like compound, Co-precipitation, Urea hydrolysis, Crystallinity, and Stacking order

## Introduction

Hydrotalcites (HTs) are a class of anionic clays also described as layered double hydroxides (LDHs). They are anionic-intercalated inorganic compounds that can be regarded as an antitype of the cationic clays like the Montmorillonite or Smectites (Geetanjali et al., 2018). Unlike the Montmorillonite or Smectites, where octahedral sheet is intruded between two tetrahedral sheets, hydrotalcites are made up of octahedral sheet introduced between two octahedral sheets. The structure is made up of different layers of two metal hydroxides joined together to form an octahedral sheet. Several of these sheets combine to form the hydrotalcite clay mineral. The octahedral metal hydroxide sheets contain two metals in different oxidation states with hydroxyl groups so arranged to form the vertices of the octahedral and metal cations at the centre (Cavani et al., 1991). The crystal structure consists of brucite-like  $\text{Mg}(\text{OH})_2$  layers (Figure 1A) with  $\text{Mg}^{2+}$  ions coordinated octahedrally by hydroxide ions sharing edges to form charged neutral sheets which are piled on each other and connected by hydrogen bonding.

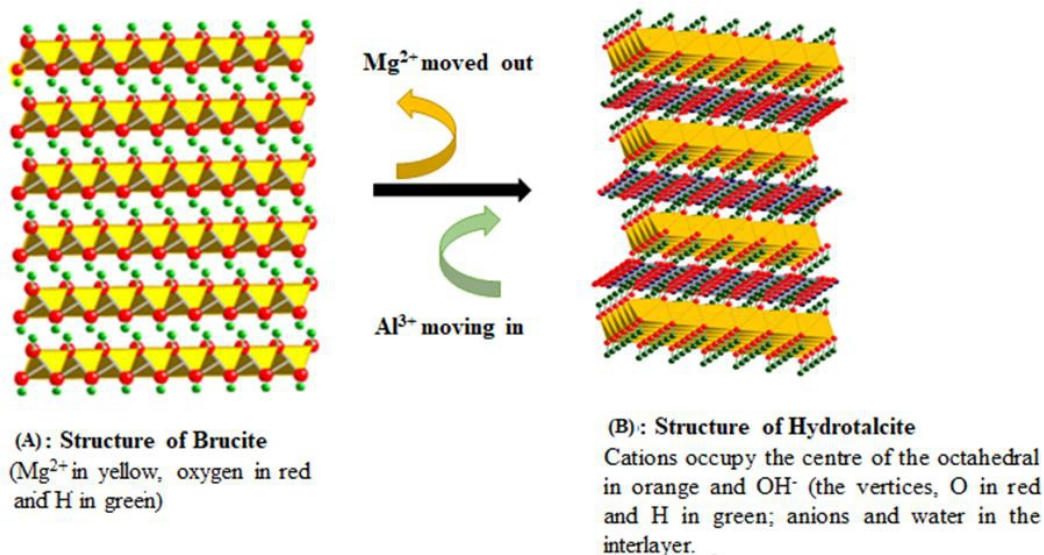


**Figure 1:** Structure of Brucite and Hydrotalcite

Isomorphic substitution of some of the  $\text{Mg}^{2+}$  ions in the brucite-like layers by trivalent cations like  $\text{Al}^{3+}$ ,  $\text{Cr}^{3+}$ ,  $\text{Fe}^{3+}$ ,  $\text{Co}^{3+}$ ,  $\text{Mn}^{3+}$  and  $\text{Ga}^{3+}$ , results in positive charge imbalance (El Hassani et al. 2017) which then allows for the existence of gallery charge balancing anions between the layers for electrical

neutrality. The remaining space in the interlayer is occupied by molecules of water of crystallisation (Figure 1. B). This group of materials were first discovered in Sweden in 1842. Manasse was the first to publish the exact formula of the hydrotalcite,  $[\text{Mg}_6\text{Al}_2(\text{OH})_{16}]\text{CO}_3 \cdot 4\text{H}_2\text{O}$  in 1915 and between 1930-1942, Feitknecht published a series of papers on double sheet structures which he termed doppelschichtstrukturen (Feitknecht and Gerber, 1942). This sprang up an increased interest in the hydrotalcite or layered double hydroxide Chemistry. Allmann and Taylor, from their single crystal x-ray diffraction results, disproved the structure that was assigned to these minerals and proposed that, these group of minerals have layers of mixed metal hydroxides intercalated with anions and water molecules (Allman, 1968 and Taylor, 1969), rather than been composed of layers of one metal hydroxide intercalated with a layer of another metal hydroxide. An extended area of compositions exist based on the general formula  $[\text{M}^{2+}_{1-x}\text{M}^{3+}_x(\text{OH})_2][\text{A}^{n-}_{x/n}] \cdot m\text{H}_2\text{O}$ , where  $\text{M}^{2+}$  and  $\text{M}^{3+}$  are di- and trivalent metals in the hydroxyl sheets with  $x$  between 0.17 and 0.33 (Cavani et al., 1991; Elgiddawy et al., 2017; Tran et al., 2018). The possibility of a number of varying types of both cationic and anionic compositions allows for tailored-made materials for diversified applications such as catalysts, adsorbents, fillers, thermal and UV radiation stabilizers etc. (Newman and Jones, 1998; Cavani et al., 1991; de Roy et al., 1992; Kuthati et al., 2015). HTs crystallise in two polymorphs (Figure 2); Rhombohedral symmetry (where the lattice parameters are  $a$  and  $c$  and  $c = 3c'$ ), and Hexagonal symmetry (where the lattice parameters are  $a$  and  $c$  and  $c=2c'$ ). For natural hydrotalcites,  $a$  and  $c$  are reported to be 3.054 and 22.81Å respectively (Drits et al., 1987), with the value of  $c'$  being 7.60Å calculated from  $d_{(003)}$  reflection (Miyata, 1983). The unit cell parameter  $a$  is the average intermetallic distance within the octahedral (cationic) layer and the unit cell  $c$  is the interlayer separation accounting for the total thickness of the metal hydroxide layer and the interlayer distance (Vaysse et al., 2002; Thomas et al., 2004; These unit cell parameters define the length of the edges of a unit cell and the angles between them.

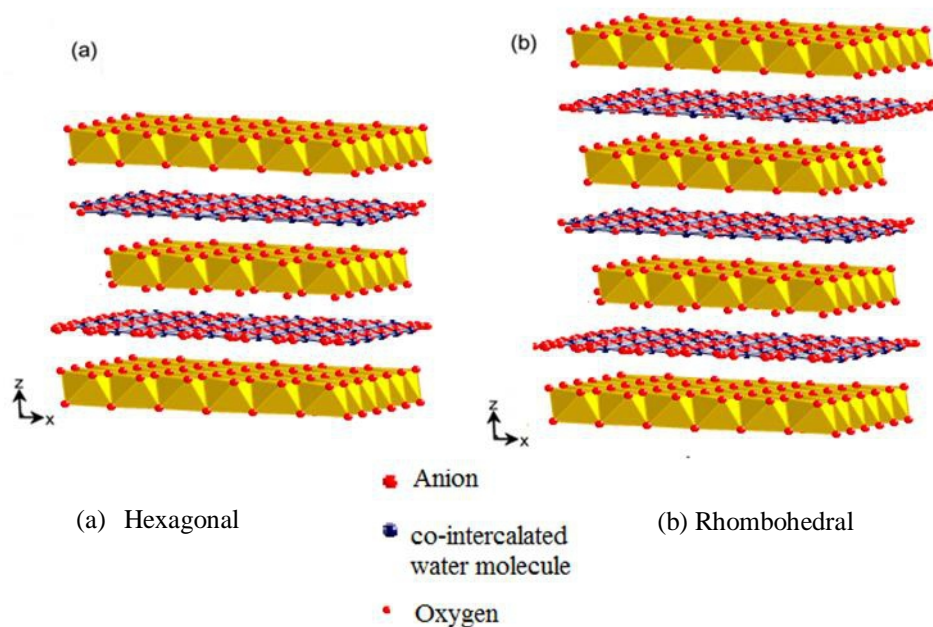


**Figure 2:** Showing the different stacking patterns of hydrotalcite

Several authors have adopted different methods to synthesise hydrotalcite-like compounds (HTlcs) such as Sol-gel method, Microwave Irradiation, Steam Activation, Solvothermal method, Co-precipitation, Urea method and Combustion Synthesis (Ross et al 1938; Costantino et al., 1998; Ogawa and Kaiho, 2002; Carreto, 2002; Carreto et al., 2006; Lvov et al., 2008), etc. The choice of method is a function of composition required and properties of the compounds desired. A commonly utilised method is the co-precipitation and the urea hydrolysis method.

The co-precipitation method is highly reliable and reproducible and it involves precipitating all cations in a controlled ratio or set by the starting solution and it includes adding steadily a solution containing the metal cations and another base usually NaOH, with a solution of the guest anion together at the same time, to a reactor with stirring and regulated flow rate.

Urea hydrolysis method involves treating the precipitated samples at moderate temperatures below and above 100°C for a few hours. It employs urea as the precipitating agent and the process proceeds slowly leading to low super saturation during the precipitation process thus giving hydrotalcite like compound with value of  $x$  of about 0.33 and good crystallinity of product. Urea is well known in gravimetric analysis where it is often used as a precipitating agent for a number of metal ions as hydroxides or as insoluble

salts from homogeneous solution in the presence of suitable anions (Mendham, 2006).

This study aims at investigating the effect of synthesis of Mg<sub>2</sub>-Al-CO<sub>3</sub> and Zn<sub>2</sub>-Al-CO<sub>3</sub>-hydrotalcite-like compounds through co-precipitation and urea hydrolysis routes and to study the effect of these routes on the physicochemical properties of the synthesised Mg<sub>2</sub>-Al-CO<sub>3</sub> and Zn<sub>2</sub>-Al-CO<sub>3</sub>-hydrotalcite-like compounds having the approximate stoichiometric formula of Mg<sub>4</sub>Al<sub>2</sub>(OH)<sub>8</sub>A<sup>n-</sup>.mH<sub>2</sub>O and Zn<sub>4</sub>Al<sub>2</sub>(OH)<sub>8</sub>A<sup>n-</sup>.mH<sub>2</sub>O where A<sup>n-</sup> is CO<sub>3</sub><sup>2-</sup>.

## Experimental

### Material

Mg(NO<sub>3</sub>)<sub>2</sub>.6H<sub>2</sub>O, 99% purity (Sigma-Aldrich, Japan), Zn(NO<sub>3</sub>)<sub>2</sub>.6H<sub>2</sub>O from Sigma-Aldrich, Germany, 98% purity, Al(NO<sub>3</sub>)<sub>3</sub>.9H<sub>2</sub>O (98% purity), Na<sub>2</sub>CO<sub>3</sub>, (98% purity) got from Sigma-Aldrich, Germany, NaOH supplied by Fisher Scientific, UK and Urea (Sigma-Aldrich, Germany, 99% purity) were utilised in this study.

### Synthesis procedure

#### Preparation of Zn/Al and Mg/Al Hydrotalcites (HTs)

Two synthesis methods were utilised to prepare hydrotalcite-like compounds (HTlcs) containing magnesium or zinc as the divalent cation, aluminium as the trivalent cation and carbonate as the interlayer anion.

Mg<sub>2</sub>-Al-CO<sub>3</sub> and Zn<sub>2</sub>-Al-CO<sub>3</sub> hydrotalcites were prepared by co-precipitation method adopted from literature (Reichle et al., 1986 and Omonmhenle and Shannon, 2016). Typically, a mixture of solutions containing aluminium and magnesium, or aluminium and zinc with Mg/Al or Zn/Al ratio of 2 having Al<sup>3+</sup> ions of 0.33M and Mg<sup>2+</sup> or Zn<sup>2+</sup> ions of 0.67M were made. Another mixed solution of NaOH [OH<sup>-</sup>] = 2M and Na<sub>2</sub>CO<sub>3</sub> [CO<sub>3</sub><sup>2-</sup>] ≈ 1M, were prepared by dissolving the compounds in de-ionised water in separate beakers. The two solutions were brought together drop wise at the same time, at constant flow rate, under vigorous stirring, maintaining the pH of the solution, 12 for Mg<sub>2</sub>-Al-CO<sub>3</sub>HTlc and 10 for Zn<sub>2</sub>-Al-CO<sub>3</sub>HTlc. When the addition was completed, the mixtures were allowed to stir for a further 1h at the same pH. The gels obtained were aged for 18h at 110°C in an autoclave. After the thermal treatment, the hydrothermal samples were filtered, washed with de-ionised water and dried at 60°C in an oven for 24 h. The solids obtained were stored in air tight containers for further analysis. The pH of the suspension was 13±0.0002 and 10.0±0.04 for Mg<sub>2</sub>-Al-CO<sub>3</sub> and Zn<sub>2</sub>-Al-CO<sub>3</sub> hydrotalcites respectively. The resulting hydrotalcite-like compounds were referred to as Mg<sub>2</sub>-Al-CO<sub>3</sub>-copptn or Zn<sub>2</sub>-Al-CO<sub>3</sub>-copptn.

Hydrotalcites like compounds of (Mg-Al and Zn-Al) were also prepared using the urea hydrolysis method following Costantino method

(Costantino et al., 1998). In a typical experiment, solid urea (1.65M) was dissolved in a solution containing the appropriate mixed metal nitrates of total concentration of 0.5M with x value of 0.33 to reach a urea/metal ion molar ratio of 3.3. The resulting clear solution was refluxed at 90°C, with constant stirring (600 rpm), for 48 h. Then the resultant gelatinous precipitates were filtered, washed and dried at 60°C for 24 h. The resulting hydrotalcite-like compounds were referred as Zn<sub>2</sub>-Al-CO<sub>3</sub>-urea or Mg<sub>2</sub>-Al-CO<sub>3</sub>-urea.

### Characterization

Powder x-ray diffraction data of as-prepared Mg<sub>2</sub>-Al-CO<sub>3</sub> hydrotalcites (by co-precipitation and urea methods) and Zn<sub>2</sub>-Al-CO<sub>3</sub> hydrotalcites (by co-precipitation and urea methods) were obtained using a Bruker D8 ADVANCE X-ray diffractometer with a Lynx-Eye PSD detector. 2 Theta transmission geometry was employed with Cu Kα<sub>1</sub> radiation ( $\lambda_{\text{CuK}\alpha_1} = 1.54056 \text{ \AA}$ ), collecting data at room temperature and at a step size of 0.02° 2θ and step time of 8s/step for routine characterization and identification of materials. The scan was carried out at diffraction angles in the 2θ range from 5° to 70°.

Thermal analysis (TG and DTA) of the samples were performed simultaneously from room temperature to 900°C in oxygen atmosphere with a Netzsch STA 449 FI Jupiter®, connected to a quadrupole mass spectrometer (Netzsch QMS 403 Aëolus®) at a heating rate of 5°C/min. The preferred products of interest that were continuously observed, were for selected mass numbers *m/z* (18) for H<sub>2</sub>O and (44) for CO<sub>2</sub>. About 50 - 60 mg of sample was heated in closed crucible (platinum), and repeated analyses were recorded for each measurement.

The atomic ratios (M<sup>II</sup>: M<sup>III</sup>) of the as-synthesised hydrotalcite like compounds were measured using a Bruker S8 TIGER x-ray fluorescence spectrometer with high intensity rhodium x-ray tube. The fused beads technique was adopted for the major oxides which involved dissolving usually 1g of sample in 10g of flux, lithium tetraborate using a platinum/gold alloy crucible at 1250°C.

The FT-IR data were collected using the ATR smart accessory on a Varian 660 Fourier transform infrared spectrometer. 36 scans were obtained for each measurement in a wavelength range of 700–4000 cm<sup>-1</sup> using 4 cm<sup>-1</sup> resolution.

## Results and Discussion

### Composition, structural and thermal analysis

The mole ratios of Mg/Al and Zn/Al in the derivatives of hydrotalcite-like compounds (HTlcs) prepared from co-precipitation and urea hydrolysis methods are shown in Table 1. The XRF results showed that mole ratio

$M^{2+}/M^{3+}$  of the synthesised samples are consistent with stoichiometry in the synthesis mixtures because the  $Mg^{2+}/Al^{3+}$  and  $Zn^{2+}/Al^{3+}$  conform well to the expected ratios in the synthesised sample, showing that the metals precipitated well.

The powder XRD patterns for  $Mg_2-Al-CO_3$  and  $Zn_2-Al-CO_3$  hydroxaltes prepared by co-precipitation and urea methods are illustrated in Figures 4 a-d. The patterns showed the characteristic lamellar structure of hydroxalite with no other phases detected indicating that, the materials synthesised consisted of one crystallised phase (Cavani et al., 1991; Trifirò and Vaccari, 1996). The lattice parameters for these samples were calculated with a hexagonal cell with rhombohedral system (Cavani et. al., 1991), and all samples show 3R symmetry, unit cell 'a' and 'c';  $\alpha = \beta = 90^\circ$  and  $\gamma = 120^\circ$ . The unit cell parameters are shown in Table 1. It was observed that  $Mg_2AlCO_3$ -co-pttn showed peak broadening around  $2\theta$ ,  $35-50^\circ$ , and relatively more intense peak with slightly bigger unit cell. While,  $Mg_2-Al-CO_3$ -urea gave slightly sharper peaks with relatively smaller unit cell. This demonstrates that the sample synthesised by the urea method showed better crystallinity, better structural order with less stacking faults and bigger particles, but denser sample from the co-precipitation method. The key difference between these preparation methods may be explained thus: in the co-precipitation method (involving hydrothermal treatment); the system is under high pressure, while often at high pressure one would expect a denser phase with small unit cell to be produced, but in this case, a denser phase with larger unit cell was observed, which may be ascribed to more water in the interlayer region of  $Mg_2-Al-CO_3$ -co-pptn. This result agrees with the TGA results, where 33.38% overall weight loss for urea sample, and greater overall weight loss of 42.38% was indeed observed for the co-precipitation samples (Figure 6). The relative better crystallinity noticed with the sample prepared by urea hydrolysis method ( $Mg_2-Al-CO_3$ -urea) may account for the differences in relative intensity and d- spacing observed (Figure 4 a).

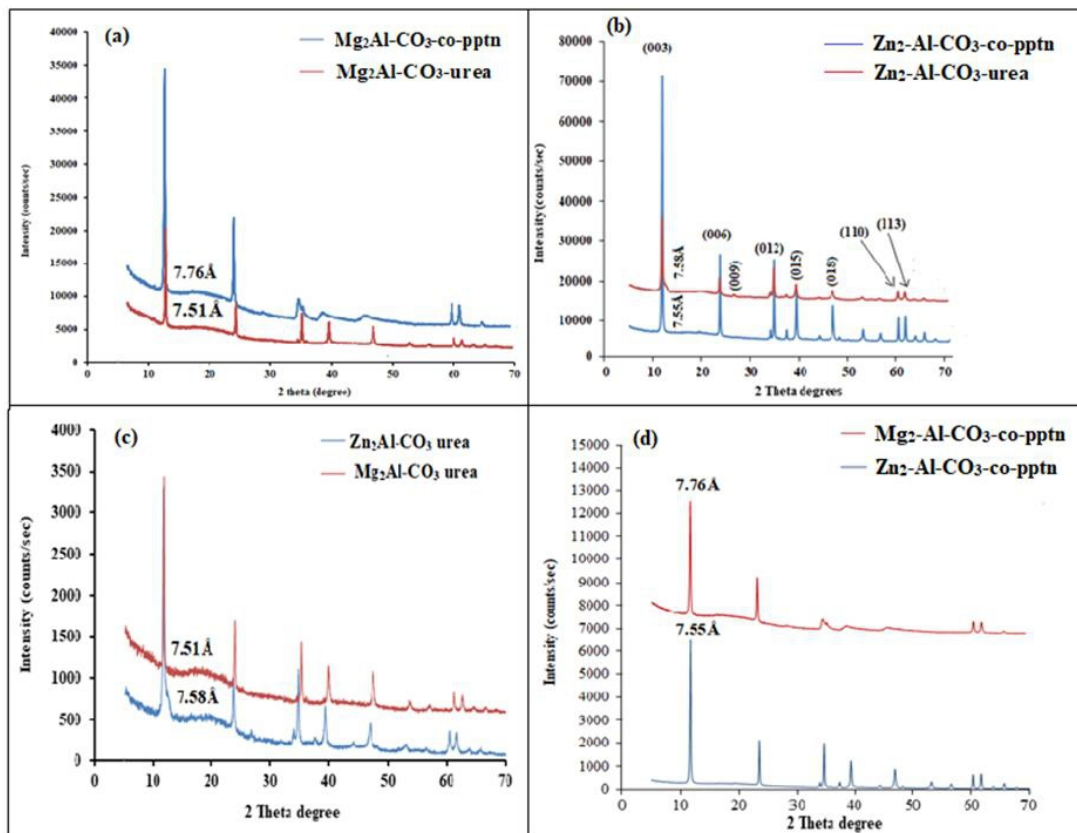


**Figure 4:** (a) Powder XRD patterns of Mg<sub>2</sub>-Al-CO<sub>3</sub>HTlc synthesised by co-precipitation and urea method, (b) Zn<sub>2</sub>-Al-CO<sub>3</sub>HTlc synthesised by urea and co-precipitation, (c) Zn<sub>2</sub>-Al-CO<sub>3</sub>HTlc and Mg<sub>2</sub>-Al-CO<sub>3</sub>HTlc synthesised by urea method and (d) Mg<sub>2</sub>-Al-CO<sub>3</sub>HTlc and Zn<sub>2</sub>-Al-CO<sub>3</sub>HTlc synthesised by co-precipitation method.

Zn<sub>2</sub>-Al-CO<sub>3</sub> hydrotalcite prepared by co-precipitation gave higher intensity and sharper peaks than Zn<sub>2</sub>-Al-CO<sub>3</sub> prepared by the urea method (Figure 4 b). Zn<sub>2</sub>-Al-CO<sub>3</sub>-co-pptn gave a denser phase with smaller unit cell (Table 1) as is expected, unlike the case of Mg<sub>2</sub>-Al-CO<sub>3</sub>-urea and Mg<sub>2</sub>-Al-CO<sub>3</sub>-co-pptn, where the opposite trend was observed (Figure 4a). The powder XRD patterns of Zn<sub>2</sub>-Al-CO<sub>3</sub> HTlc and Mg<sub>2</sub>-Al-CO<sub>3</sub> prepared by urea hydrolysis method are shown in Figure 4 c. The powder XRD patterns are similar and both demonstrate that their layered structures are very similar. The  $d_{(003)}$  reflection of Zn<sub>2</sub>-Al-CO<sub>3</sub>-urea is observed at approximately ca.7.58Å, corresponding to a unit cell parameter  $c$  of ca.22.73Å while for Mg<sub>2</sub>-Al-CO<sub>3</sub>-urea, it is observed at ~7.51Å corresponding to a unit cell parameter  $c$  of ca.22.53Å. Mg<sub>2</sub>-Al-CO<sub>3</sub>-urea also showed sharper peaks indicating relatively better crystallinity, which may be an indication of better order. Comparing both samples, powder XRD patterns of Zn<sub>2</sub>-Al-CO<sub>3</sub>-co-pptn and Mg<sub>2</sub>-Al-CO<sub>3</sub>-

co-pptn are shown in Figure 4 d.  $Zn_2-Al-CO_3$ -co-pptn showed relatively sharper peaks with smaller unit cell, and the peak broadening observed around  $2\theta$ ,  $35-50^\circ$  in  $Mg_2-Al-CO_3$ -co-pptn is not present. This suggests better crystallinity, better structural order with less stacking faults with  $ZnAlCO_3$ -co-pptn.

**Table 1:** Unit cell parameters and mole ratios of the various as-synthesised hydroxalicates

Hydroxalcite Sample	Cations mole ratio	<i>a</i> (Å)	<i>c</i> (Å)	<i>d</i> <sub>(003)</sub> (Å)	<i>d</i> <sub>(006)</sub> (Å)	<sup>a</sup> <i>M</i> <sup>2+</sup> / <i>M</i> <sup>3+</sup> ratio (Experimental)
$Mg_2-Al-CO_3$ by co-pptn method	Mg/Al 2:1	3.0438(71)	23.2675(40)	7.7554	3.8777	2.36:1
$Mg_2-Al-CO_3$ by urea hydrolysis method	Mg/Al 2:1	3.0269(11)	22.5340(14)	7.5113	3.7557	2.04:1
$Zn_2-Al-CO_3$ by co-pptn method	Zn/Al 2:1	3.0679(11)	22.6419(4)	7.5474	3.7737	2.18:1
$Zn_2-Al-CO_3$ by urea method	Zn/Al 2:1	3.0708(13)	22.7261(6)	7.5754	3.7877	2.07:1

Unit cell parameters calculated with celref software using hexagonal crystal system; <sup>a</sup>*M*<sup>2+</sup>/*M*<sup>3+</sup> ratios in the synthesised hydroxalicates by x-ray fluorescent analysis; co-pptn = co-precipitation method.

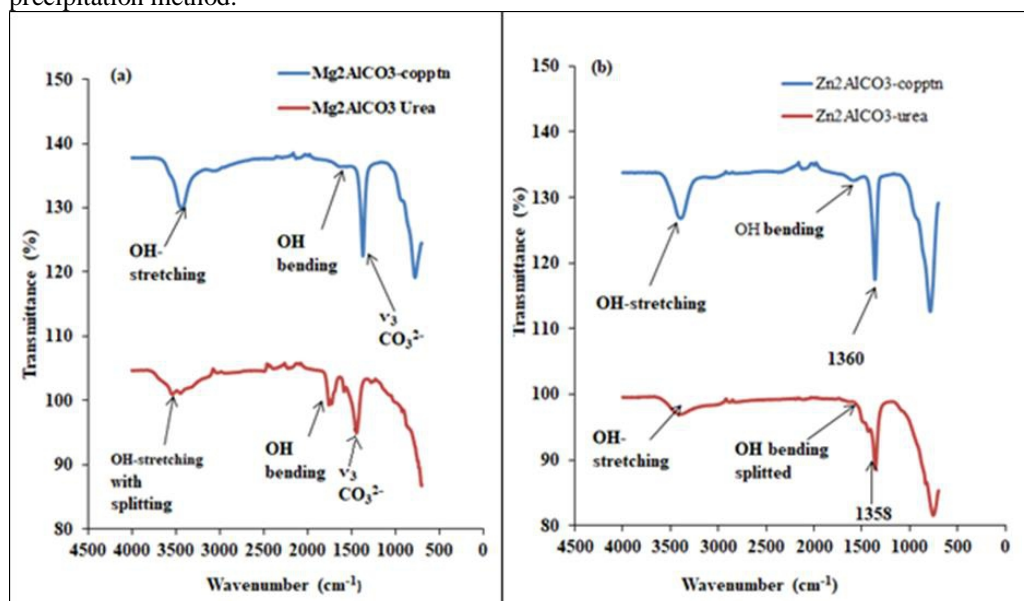


**Figure 5:** FT-IR spectra of (a)  $Mg_2-Al-CO_3$  hydroxalcite-like compounds synthesised by co-precipitation and by urea hydrolysis method and (b)  $Zn_2-Al-CO_3$  hydroxalcite-like compounds synthesised by co-precipitation and by urea

The FT-IR spectra in the region between  $700 - 4000\text{ cm}^{-1}$  for  $Mg_2-Al-CO_3$  and  $Zn_2-Al-CO_3$  hydroxalcite-like compounds synthesised by co-precipitation and by urea method are shown in Figure 5. The broad peaks around  $3400\text{ cm}^{-1} - 3600\text{ cm}^{-1}$  for each of the samples are ascribed to the water hydroxyl stretching vibrations of the hydroxide layers and interlayer water

molecules. The bands between 1620 and 1656 $\text{cm}^{-1}$  corresponding to bending vibration of interlayer water.  $\text{Mg}_2\text{-Al-CO}_3\text{HTlc}$  by urea route shows splitting of this OH bending band (Figure 5 a, lower spectrum), which may suggest stronger hydrogen bonding and better ordering of cations within the hydroxide octahedral layers and the interlayer region. Furthermore, there is relative shifting of this band to lower frequency which may be due to greater order of the  $\text{CO}_3^{2-}$  anions and water molecules in the interlayer space. These results agree with the XRD result.

The sharp bands around 1340-1365 $\text{cm}^{-1}$  are ascribed to gallery carbonate anions for both samples. Relatively, the absorption band due to the carbonate anion in the  $\text{Mg}_2\text{-Al-CO}_3\text{HTlc}$  by co-precipitation method (Figure 5a upper spectrum) shows sharper and more intense band and this is consistent with the pXRD results, showing this sample as having denser overall packing. The sharp intense vibration bands observed around 1367 $\text{cm}^{-1}$  ( $\text{Mg}_2\text{-Al-CO}_3\text{-co-pptn}$ ) and 1365  $\text{cm}^{-1}$  ( $\text{Mg}_2\text{-Al-CO}_3\text{-urea}$ ) indicate  $\text{CO}_3^{2-}$  from  $\nu_3(\text{CO}_3^{2-})$  and is a confirmation of the intercalation of carbonate in the interlayer spaces of these samples.  $\text{Mg}_2\text{-Al-CO}_3$  prepared by both co-precipitation and urea method respectively, each possess a shoulder around higher frequency region. This may have been caused by increased interaction involving hydrogen bonding between the  $\text{OH}^-$  on the layers,  $\text{CO}_3^{2-}$  anions and  $\text{H}_2\text{O}$  molecules situated in the interlayer space. This hydrogen bonding effect is stronger in the  $\text{Mg}_2\text{-Al-CO}_3\text{ HTlc}$  synthesised by the urea method typified by the degenerates observed around 3300-3500 $\text{cm}^{-1}$  suggesting stronger Mg-Al hydroxide layer and interlayer interactions, and long range order. This is supported by XRD results (Figure 4). However, the contamination of this sample by a little amount of urea during synthesis cannot be ruled out because of the following observations; splitting observed around 3250-3500 $\text{cm}^{-1}$ , and the appearance of the band observed around 1580 $\text{cm}^{-1}$ , which may be as a result of vibration bands due to  $\text{NH}_2$  from urea. The weak broad band's presented around 1640-1660 $\text{cm}^{-1}$  are ascribed to the water bending vibration. The significant variations in the band positions of the spectra of these samples may be due to a possibility of differences in order/disorder existing in the orderly pile of the layers.

The FT-IR spectra of  $\text{Zn}_2\text{-Al-CO}_3$  hydrotalcite-like compounds through urea and co-precipitation routs are showed in Figure 5b. The absorption peaks at 754 $\text{cm}^{-1}$  for  $\text{Zn}_2\text{-Al-CO}_3$  by urea and 779 $\text{cm}^{-1}$  for  $\text{Zn}_2\text{-AlCO}_3$  by co-precipitation method are related to the metal-oxygen  $\nu(\text{M-O-M})$  thus confirming the structure of a layered double hydroxide. The peaks located at about 1358  $\text{cm}^{-1}$  ( $\text{Zn}_2\text{-Al-CO}_3$  by urea) and 1360  $\text{cm}^{-1}$  ( $\text{Zn}_2\text{-Al-CO}_3$  by co-pptn) is attributed to O-C-O stretching vibrations of the carbonate anions which confirm the presence of  $\text{CO}_3^{2-}$  as the intercalated anion in the interlayer regions. There are also significant variations in the band positions of the

spectra of these samples which may be attributed to a possibility of differences in order/disorder existing in the stack up of the layers, and hydrogen bonding between the carbonate ions in the interlayer region and the hydroxyl ions of the metal hydroxide layers.

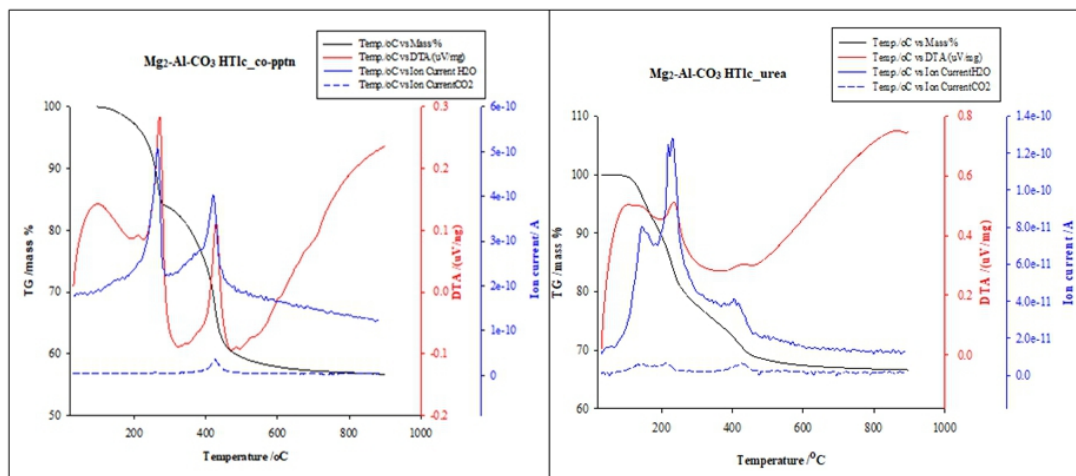


**Figure 6:** TG, DTA and gas evolution ion current curves of (Left)  $Mg_2-Al-CO_3$ HTlc by coprecipitation and (right)  $Mg_2-Al-CO_3$ HTlc by urea. TGA% (Black); DTA/ $\mu V/mg$  (Red); ion current curve for  $H_2O$  m18 100% (Blue line ); ion current curve for  $CO_2$  m44 94.7% (blue broken line). TGA (left vertical axis) and its derivative (right vertical axis)

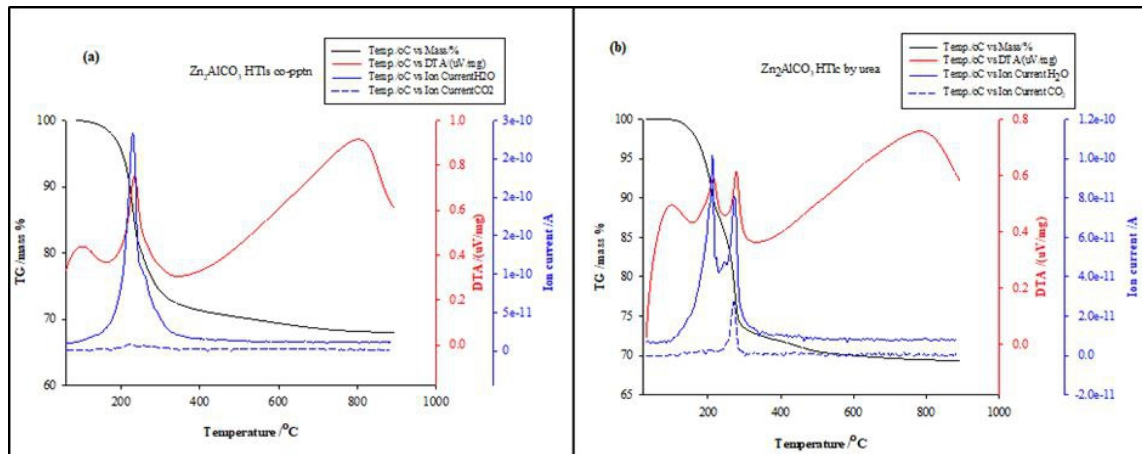


**Figure 7:** TG, DTA and gas evolution ion current curves of (a)  $Zn_2-Al-CO_3$ HTlc by coprecipitation (b)  $Zn_2-Al-CO_3$ HTlc by urea. TGA% (Black); DTA/ $\mu V/mg$  (Red); ion current curve for  $H_2O$  m18 100% (Blue ); ion current curve for  $CO_2$  m 44 94. 71% (blue broken line). TGA (left vertical axis) and its derivative (right vertical axis)

Thermogravimetric analysis measurements were carried out to investigate the phase changes during the thermal analysis of the derivatives of the two route products,  $Mg_2-Al-CO_3$  and  $Zn_2-Al-CO_3$  hydrotalcite. The first wt. loss occurred at lower temperature below  $280^\circ C$  (precisely between 40-

280°C) and can be attributed to the removal of water from the interior of the gallery surfaces and also water physiosorbed on the external sample surfaces. The ion current curve showed that water was removed from Mg<sub>2</sub>-Al-CO<sub>3</sub>-co-pptn (Figure 6b) at ca. 266°C accounting for 16% weight loss. The second weight loss step occurred at higher temperature as a result of withdrawal of water from the metal hydroxide layers (loss of hydroxyl group) as well as breakdown of the carbonate anion present in the interlayer space to release CO<sub>2</sub>. The ion current curve shows that Mg<sub>2</sub>-Al-CO<sub>3</sub>-co-pptn lost water at 422°C and CO<sub>2</sub> gas at 424°C. This process accounts for a wt loss of 23.5%. The total weight loss at 900°C is thus 43.4%.

Thermal analysis of Mg<sub>2</sub>-Al-CO<sub>3</sub>-urea is shown in Figure 6a. The thermal analysis of this sample basically followed the same trend as in Mg<sub>2</sub>-Al-CO<sub>3</sub>-co-pptn. It shows a total mass loss of 33.4%. The first wt. loss was observed to occur between 40-240°C. The DTA shows a broad endothermic peak centered at 105°C and another, a little less broad peak at 233°C. The ion current curves showed that water was lost in two steps, first at ca. 146°C and secondly at 234°C. The other wt. loss involving the simultaneous removal of interlayer carbonate, water and abstraction of hydroxyl groups from the brucite-like layers occurred at ca. 432°C.

The DTA curve for Zn<sub>2</sub>-Al-CO<sub>3</sub>-co-pptn clearly shows three endothermic peaks (Figure 7a). The first change that occurs during thermal analysis of this sample is associated with the removal of water physiosorbed on the surfaces of the hydrotalcite and from the interior surfaces of the gallery and this happened around 90-140°C, followed by the second step involving simultaneous abstraction of water from the layers and carbonate from the internal galleries leading to collapse of the structure. This step and the former may have overlapped and is represented on the DTA by the endothermic peak centered at 235°C (Figure 7a). The mass spectrometry analysis showed the evolution of H<sub>2</sub>O in a single step at 231°C and CO<sub>2</sub> at 225°C. Total weight losses of 32% were observed.

For the Zn<sub>2</sub>-Al-CO<sub>3</sub>-urea sample, the weight losses observed in the TG curve are slightly better resolved, due to improved order, though the same trend of thermal behaviour was observed. Here the first process is represented by two endothermic peaks on the DTA centered at ca. 101°C and 216°C. This accounts for 12% wt. loss. The mass spectrometry analysis shows that water was released at ca. 211°C. The other wt. loss step is centered at ca.278°C and it represents the process in which the sample starts to crumble due to loss of carbonate (at ca.271°C) from within the galleries, and abstraction of water (at ca. 274°C) from the layers. This step accounts for 19% wt. loss, with a total wt. loss of 31%.

The point at which this material loses water from the layers and interlayer's and, at the same time losing the intercalated carbonate anions and

then collapsing, can be taken as an indication for thermal stability. A delay in dehydroxylation of the layers demonstrates a more stable hydrotalcite-like compound. Therefore, thermal stability is follows thus:  $Zn_2-Al-CO_3$ -urea <  $Zn_2-Al-CO_3$ -co-pptn <  $Mg_2-Al-CO_3$ -urea <  $Mg_2-Al-CO_3$ -co-pptn. The stability of derivatives of co-precipitation is more stable than the derivatives of urea method and  $Zn_2-Al-CO_3$  is less stable than its  $Mg-Al-CO_3$  counterparts.

## Conclusion

$Mg_2-Al-CO_3$  and  $Zn_2-Al-CO_3$  hydrotalcite-like compounds have been synthesised via co-precipitation and urea routes. The synthesised samples conform to  $M^{3+}/M^{3+}+M^{2+}$  value of approximately 0.33 consistent with stoichiometric in the synthesis solutions. Variation in synthesis route can lead to possibility of differences in order/disorder present in the stacking of the layers, order of the carbonate anions and water molecules in the interlayer space and hydrogen bonding between the carbonate ions and the hydroxyl ions of the metal hydroxide layers. The urea hydrolysis yielded  $Mg_2-Al-CO_3$  hydrotalcite with better crystallinity and structural order than its co-precipitation counterpart which showed denser particles and bigger unit cell. On the other hand,  $Zn_2-Al-CO_3$  hydrotalcite showed the reverse trend that's naturally expected. The derivatives of co-precipitation method are more stable than the derivatives of urea method. And  $Zn_2-Al-CO_3$  is less stable than its  $Mg-Al-CO_3$  counterparts.

## Acknowledgment

The authors thank TET fund Nigeria (SIO is a recipient of its grant), and Birmingham Science city: creating and characterising new generation advanced materials (West Midlands Centre for Advanced Material Project 1), with (AWM) and (ERDF).

## References:

1. Allmann, R., (1968). The Crystal Structure of Pyroaurite, *Acta Crystallography Section. B*, 24 (7), pp 972-977. doi.org/10.1107/S0567740868003511
2. Carretero, M. I. (2002). Clay Minerals and their Beneficial Effects upon human health. A review. *Applied Clay Science*, 21(3-4), pp 155-163. doi.org/10.1016/S0169-1317(01)00085-0
3. Carretero, M. I., Gomes, C. S. F., and Tateo, F. (2006). 5 Clays and human health. *Developments in clay science*, 1, pp 717-741. doi.org/10.1016/S1572-4352(05)01024-X
4. Cavani, F, Trifirò F, Vaccari A. (1991). Hydrotalcite-type anionic clays: Preparation, properties and applications. *Catalysis Today*, 11(2), pp 173-301. doi.org/10.1016/0920-5861(91)80068-K

5. Costantino, U., Marmottini, F., Nocchetti, M., Vivani, R., 1998. New Synthetic Routes to Hydrotalcite-Like Compounds– Characterisation and Properties of the Obtained Materials. *European Journal of Inorganic Chemistry*, 1998(10), pp.1439-1446. doi:10.1002/(sici)1099-0682(199810)1998:10<1439::aid-ejic1439>3.0.co;2-1
6. De Roy, A., Forano, C., El Malki, K., Besse JP. (1992) Anionic Clays: Trends in Pillaring Chemistry. In: Ocelli M.L., Robson H.E. (eds) *Expanded Clays and Other Microporous Solids*. pp. 108-169, Springer, Boston, MA. doi.org/10.1007/978-1-4615-3534-8\_7
7. El Hassani, K., Beakou, B.H., Kalnina, D., Oukani, E., Anouar A. (2017). Effect of morphological properties of layered double hydroxides on adsorption of azo dye methyl orange: A comparative study. *Applied Clay Science* 140, pp 124–131. doi.org/10.1016/j.clay.2017.02.010
8. Elgiddawy, N, Essam, T.M., El Rouby, Raslam, M., Farghali, A.A. (2017). New approach for enhancing *Chlorella vulgaris* biomass recovery using ZnAl-layered double hydroxide nanosheets. *Journal Applied Phycology* 29 (3), pp 1399-1407. doi: 10.1007/s10811-017-1050-5
9. Feitknecht, W., Gerber, M. (1942). Zur Kenntnis der Doppelhydroxyde und basischen Doppelsalze III. Über Magnesium Aluminium doppel hydroxyd. *Helvetica Chimica Acta*, 25(1), pp 131-137. doi.org/10.1002/hlca.19420250115
10. Geetanjali, M., Barsha, D., Sony, P. (2018). Layered double hydroxides: A brief review from Fundamentals to Application as evolving biomaterials, *Applied Clay Science*, 153, pp172-186. doi.org/10.1016/j.clay.2017.12.021
11. Jepson, W. B. (1984). Kaolins: Their Properties and Uses. *Philosophical Transactions of the Royal Society A: Mathematical, Physical and Engineering Sciences*, 311 (1517), pp 411–432. doi:10.1098/rsta.1984.0037
12. Kopka, H., Beneke, K., Lagaly, G. (1988). Anionic Surfactants between Double Metal Hydroxide Layers, *Journal of Colloid and Interface Science*. Vol. 123, No. 2. pp 427-436. doi.org/10.1016/0021-9797(88)90263-9
13. Kuthati, Y., Kankala, R.K., Lee, C. H. (2015). Layered double hydroxide nanoparticles for biomedical applications: Current status and recent prospects. *Applied Clay Science*, 112, 100-116. doi.org/10.1016/j.clay.2015.04.018

14. Lvov, Y. M., Shchukin, D. G., Mohwald, H., & Price, R. R. (2008). Halloysite clay nanotubes for controlled release of protective agents. *ACS Nano*, 2(5), 814-820. doi: 10.1021/nm800259q
15. Manasse, E. (1915). Rocceeritree e di adencollezioneissel, Attidella Societal Toscana di Scienze Naturali, In Processi Verballi, 24, pp92.
16. Miyata, S., (1983). Anion-Exchange Properties of Hydrotalcite-Like Compounds, *Clays and Clay Minerals*, 31, pp 305-311. doi: 10.1346/ccmn.1983.0310409
17. Newman, S.P., Jones, W. (1998). Synthesis, characterization and applications of layered double hydroxides containing organicguests. *New Journal of Chemistry*, 22, (2), pp 105-115. doi:10.1039/a708319j
18. Reichle, W. (1986). The nature of the thermal decomposition of a catalytically active anionic clay mineral. *Journal of Catalysis*, 101(2), 352–359. doi:10.1016/0021-9517 (86) 90262-9
19. Ross, C. S., Kerr, P. F. (1934). *Halloysite and allophane*. US Government Printing Office. <https://pubs.usgs.gov/pp/0185g/report.pdf>
20. Taylor, H.F.W. (1969). Segregation and Cation-Ordering in sjögrenite and pyroaurite, *Mineralogical Magazine* 37 (287), pp 338-342. doi:10.1180/minmag.1969.037.287.04
21. Tran, Hai Nguyen, Lin, Chu-Ching, Woo, Seung Han, Chao, Huang-Ping (2018). Efficient removal of Copper and lead by Mg/Al Layered double hydroxides intercalated with organic acid anions: adsorption kinetics, isotherms, and thermodynamic. *Applied Clay Science*, 154, pp 17-27. doi.org/10.1016/j.clay.2017.12.033
22. Trifiro, F., Vaccari, A. (1996). *Comprehensive Supramolecular Chemistry*, JL Atwood, JED Davies, DD Mc Nicol, F. Vögtle (eds), 7, Pergamon, Oxford.
23. V. A. Drits, T. N. Sokolova, G. V. Sokolova, and V. I. Cherkashin. (1987). New Members of the Hydrotalcite-Manasseite Group, *Clays and Clay Minerals*, 35 (6), pp 401-417. doi: 10.1346/ccmn.1987.0350601
24. Velde, B. (1992), Introduction to Clay Minerals: Chemistry, Origin, Uses and Environmental Significance, London, Chapman and Hall.
25. Mendham, J., (2006). Vogel's textbook of quantitative chemical analysis, Pearson Education, India.